

Electron transfer catalysis in the activation of C–H bonds by ruthenium complexes

Antonio Ceccanti^a, Pietro Diversi^{b,*}, Giovanni Ingrosso^b, Franco Laschi^a,
Antonio Lucherini^b, Stefania Magagna^b, Piero Zanello^a

^a Dipartimento di Chimica, Università di Siena, Pian dei Mantellini 44, 53100 Siena, Italy

^b Dipartimento di Chimica e Chimica Industriale, Università di Pisa, Via Risorgimento 35, 56126 Pisa, Italy

Received 13 March 1996; revised 31 May 1996

Abstract

Ruthenium(II) dimethyl complexes, $[\text{Ru}(\text{Me})_2(\eta^6\text{-C}_6\text{Me}_6)(\text{PR}_3)]$ ($\text{R} = \text{Ph}$ **1a**, $\text{R}_3 = \text{MePh}_2$ **1b**, $\text{R}_3 = \text{Me}_2\text{Ph}$ **1c**, $\text{R} = \text{Me}$ **1d**, $\text{R} = \text{Et}$ **1e**), react with C–H bonds of benzene or toluene under severe conditions (85–105 °C depending on the phosphine ligand) to give methane and the new methyl aryl derivatives $[\text{Ru}(\text{Me})(\text{Ar})(\eta^6\text{-C}_6\text{Me}_6)(\text{PR}_3)]$. The methyl tolyl complexes are formed as a 2/1 mixture of meta and para isomers. In contrast the reaction of **1a–1e** with arenes, in the presence of $[\text{FeCp}_2]\text{PF}_6$, proceeds rapidly at room temperature: the corresponding methyl aryl derivatives $[\text{Ru}(\text{Me})(\text{Ar})(\eta^6\text{-C}_6\text{Me}_6)(\text{PR}_3)]$ ($\text{Ar} = \text{Ph}$, Tol) and/or the intramolecular reaction products $[\text{Ru}(\text{C}_6\text{H}_4\text{PR}_2)(\text{Me})(\eta^6\text{-C}_6\text{Me}_6)]$ are formed depending on the steric hindrance of the phosphine. The fact that electrochemistry and ESR spectroscopy show that on oxidation the ruthenium(II) complexes give stable ruthenium(III) congeners suggests that the catalytic reaction triggered by ferrocenium ions proceeds through a different redox pathway.

Keywords: Ruthenium–hexamethylbenzene complexes; C–H activation; Electron transfer behaviour

1. Introduction

We have recently found that the iridium dimethyl complexes $[\text{Ir}(\text{Me})_2\text{Cp}^*(\text{PR}_3)]$ ($\text{Cp}^* = \text{C}_5\text{Me}_5$, $\text{R} = \text{Ph}$, Me), which are able to activate C–H bonds of arenes only under rather drastic conditions or not at all, become strongly reactive in the presence of catalytic amounts of one-electron oxidants [1–3]. These C–H activation reactions have features which make them analogous to the ‘ σ -bond metathesis’ [4] of M–R bonds and hydrocarbons C–H bonds (Eq. (1)).



This reaction had been previously observed for early transition or f-block [4], and for a few late transition metals [5,6] under conditions of thermal activation. We decided to study the reactivity of the half-sandwich d⁸ ruthenium system $[\text{Ru}(\text{Me})_2(\eta^6\text{-C}_6\text{Me}_6)(\text{L})]$ ($\text{L} =$ phosphine) with arenes, both under thermal and oxidative conditions, in order to test the generality of the

electron transfer catalysis already observed for the iridium dimethyl derivatives. The results of this study are reported here.

2. Results and discussion

2.1. Synthesis of the ruthenium dimethyl complexes **1a–1e**

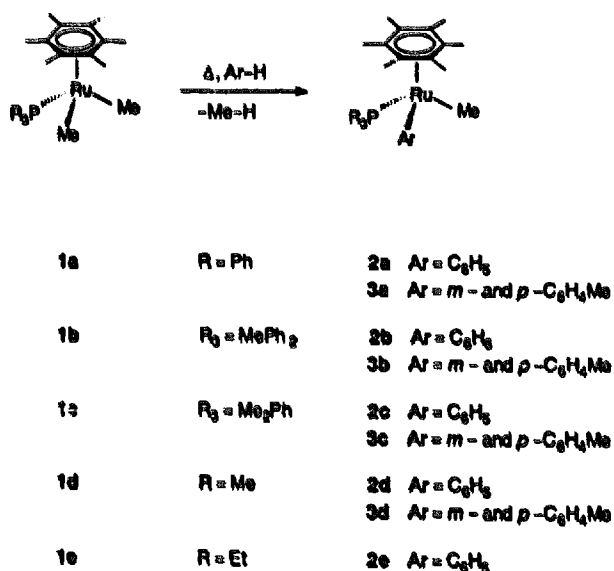
The ruthenium(II) dimethyl complexes, $[\text{Ru}(\text{Me})_2(\eta^6\text{-C}_6\text{Me}_6)(\text{PR}_3)]$ ($\text{R} = \text{Ph}$ **1a**, $\text{R}_3 = \text{MePh}_2$ **1b**, $\text{R}_3 = \text{Me}_2\text{Ph}$ **1c**, $\text{R} = \text{Me}$ **1d**, $\text{R} = \text{Et}$ **1e**) have been synthesized with some modification of the literature method reported for **1a**, **1b** and **1d** [7], by reacting the corresponding dichloro derivatives with methyl lithium. As far as we know, **1c** and **1e** were not previously reported. In all cases the reaction mixture was hydrolysed at 0 °C in order to eliminate the excess of the alkylating agent: attempted crystallization of the dimethyl derivatives without prior elimination of the excess of LiMe from the reaction mixture was unsuccessful. Purification by column chromatography on alu-

* Corresponding author. Tel.: (+39) 50 918225; fax: (+39) 50 918260; e-mail: div@ccci.unipi.it.

mina was found to be a suitable route, although with some inconveniences. While **1a** and **1b** were successfully purified, **1c–1e** were found to decompose extensively by using a 7 cm long column. In particular, by chromatography of **1d** on alumina an orange-yellow band was eluted by chloroform, which was identified as $[\text{Ru}(\text{Me})(\text{Cl})(\eta^6\text{-C}_6\text{Me}_6)(\text{PMe}_3)]$. This compound is most probably originated by protonolysis of one of the Ru–Me bonds by the OH groups on the alumina surface, followed by metathesis with chloride ion impurities. A similar observation had been made previously in our laboratory during attempted purification of $[\text{Ru}(\text{CH}_2\text{CMe}_2\text{CH}_2)(\eta^6\text{-C}_6\text{Me}_6)(\text{PR}_3)]$ (R = Me, Ph) by column chromatography on alumina, which gave on chloroform elution the orthometallated derivative $[\text{Ru}(\text{C}_6\text{H}_4\text{PRPh})(\text{Cl})(\eta^6\text{-C}_6\text{Me}_6)(\text{PR}_3)]$ [8]. However, **1c–1e** were satisfactorily purified by fast chromatography through a short alumina column.

2.2. Thermolysis of **1a–1e** in the presence of arenes

The reactivity of **1a–1e** towards arenes has been studied under conditions of thermal activation. All these compounds are able to activate benzene C–H bonds giving methane and the methyl phenyl complexes **2a–2e** (Scheme 1) at temperatures higher than 85 °C, although some dissociation of hexamethylbenzene followed by decomposition is observed. Structural assignments were made by ^1H NMR spectroscopy and by comparison with authentic samples prepared by a different route (see Section 4 and Table 1). The temperatures of thermolysis, which result from a compromise between a convenient rate of the C–H activation and reasonably low decomposition of the complexes, depend upon the nature of the phosphine: **2a** and **2b**, 85 °C; **2c**, 100 °C; **2d**, 110 °C; **2e**, 90 °C.



Scheme 1.

Reactions with benzene-*d*₆ have been followed by ^1H NMR spectroscopy and, in the case of **1a**, a reasonably good pseudo first-order kinetic law for over four half-lives ($k = 4.33 \times 10^{-2} \text{ h}^{-1}$, $t_{1/2} = 16 \text{ h}$, $85 \pm 0.5^\circ\text{C}$) is observed. In all other cases decomposition becomes so important that a simple kinetic law can hardly be evaluated. Since there is no experimental evidence for intramolecular activation steps (no MeH and no orthometallated product have been detected), we suggest the formation of a reaction intermediate deriving from the temporary loss of the phosphine. This is consistent with the complete inhibition of the reaction by an excess of free phosphine in the case of **1a** ($\text{PPh}_3/\mathbf{1a} = 3$), and with the increasing thermolysis temperature in the order **1a** < **1b** < **1c** < **1d**, which agrees nicely with the cone angle decreasing [9]. Analogously, Maitlis and coworkers [5] have proposed that for the arene thermal activation reactions by the related complex $[\text{Ir}(\text{Me})_2\text{Cp}^*(\text{DMSO})]$ (DMSO = dimethylsulphoxide), the loss of the DMSO ligand is a prerequisite for the oxidative addition of the arene C–H bond.

1a–1e are also able to activate toluene, which reacts more slowly than benzene: 90% conversion has been attained at 85 °C after 50 h in the case of the reaction of **1a** with benzene, while more than 600 h are necessary at 110 °C in order to reach the same conversion in the case of the reaction of **1a** with toluene ($k = 1.15 \times 10^{-2} \text{ h}^{-1}$, $t_{1/2} = 60 \text{ h}$ for the reaction with toluene-*d*₈). In all cases the reaction products are a 2/1 mixture of the *m*- and *p*-tolyl derivatives (Scheme 1). The two isomers were identified by analysis of the ^1H NMR spectra of the reaction mixtures, and by analogy with the iridium(III) systems [1–3]. There is no evidence for activation of ortho- and benzylic C–H bonds.

2.3. Oxidatively promoted arene C–H activation by **1a–1d**

Treatment of **1a** with benzene in the presence of small amounts (30%) of $[\text{FeCp}_2]\text{PF}_6$ produces, after an induction period of a few seconds, a rapid evolution of gas at the solid–oxidant surface. Monitoring the reaction by ^1H NMR, we have observed the formation of ferrocene, CH₄ and, after 24 h, the total conversion of **1a** into two organometallic compounds, as shown by the new signals of coordinated C₆Me₆. The major compound (65%) has been isolated and identified as the orthometallated complex $[\text{Ru}(\text{C}_6\text{H}_4\text{PPh}_2)(\text{Me})(\eta^6\text{-C}_6\text{Me}_6)]$ (**4a**) (Scheme 2). In fact the aromatic region of the ^1H NMR spectrum shows the typical pattern of the orthometallated triphenylphosphine, the high field resonance in the ^{31}P NMR spectrum ($\delta = -10.79$ in benzene-*d*₆) being consistent [10] with the presence of a phosphorus atom in a four-membered ring (Table 1). We were not able to isolate the minor organometallic

Table 1
¹H NMR data ^a

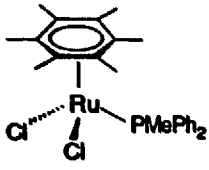
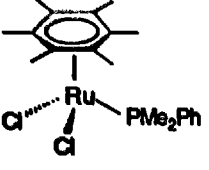
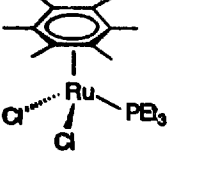
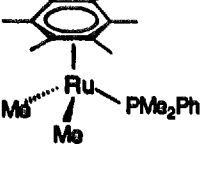
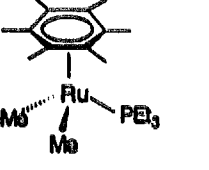
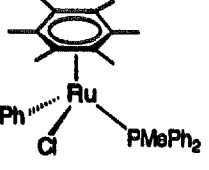
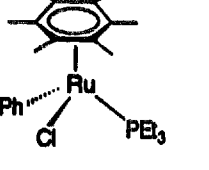
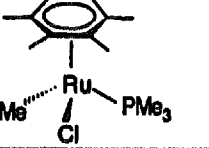
Compound	¹ H NMR
	1.74 (18H, d, $J_{HP} = 0.7$ Hz, C_6Me_6), 1.89 (3H, d, $J_{HP} = 10.8$ Hz, PMe), 7.35–7.45 (6H, m, H_m , H_p), 7.7–7.8 (4H, m, H_o). ^b
	1.69 (6H, d, $J_{HP} = 10.8$ Hz, PMe), 1.77 (18H, d, $J_{HP} = 0.7$ Hz, C_6Me_6), 7.35–7.45 (3H, m, H_m , H_p), 7.7–7.8 (2H, m, H_o). ^b
	0.92 (9H, dt, $J_{HP} = 14.3$ Hz, $J_{HH} = 7.6$ Hz, PCH_2Me), 1.67 (18H, s, C_6Me_6), 1.81 (6H, dq, $J_{HP} = 9.6$ Hz, $J_{HH} = 7.6$ Hz, PCH_2Me). ^b
	0.08 (6H, d, $J_{HP} = 6.5$ Hz, RuMe), 1.24 (6H, d, $J_{HP} = 8.2$ Hz, PMe), 1.55 (18H, s, C_6Me_6), 7.0–7.4 (5H, m, PPh_3).
1c	
	-0.6 (6H, d, $J_{HP} = 5.4$ Hz, RuMe), 0.82 (9H, dt, $J_{HP} = 7.6$ Hz, $J_{HH} = 13.4$ Hz, PCH_2Me), 1.47 (6H, m, PCH_2Me), 1.73 (18H, s, C_6Me_6).
1e	
	1.62 (3H, d, $J_{HP} = 9.0$ Hz, PMe), 1.53 (18H, s, C_6Me_6), 6.9–7.6 (15H, m, Ph).
	0.81 (9H, m, PCH_2Me), 1.5–1.9 (6H, m, PCH_2Me), 1.63 (18H, s, C_6Me_6), 7.0–7.3 (5H, m, Ph).
	0.70 (3H, d, $J_{HP} = 8.0$ Hz, RuMe), 1.08 (9H, d, $J_{HP} = 10.0$ Hz, PMe), 1.68 (18H, s, C_6Me_6).

Table 1 (continued)

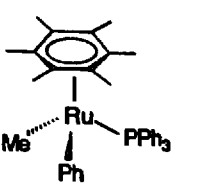
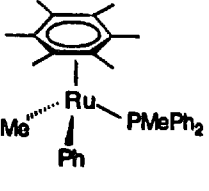
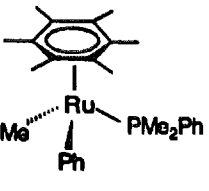
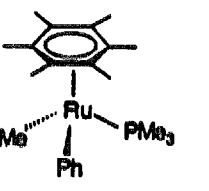
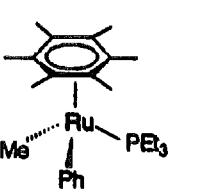
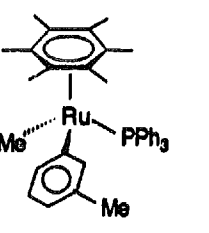
Compound	¹ H NMR
	0.39 (3H, d, $J_{HP} = 7.5$ Hz, RuMe), 1.53 (18H, s, C_6Me_6), 6.9–7.5 (20H, m, Ph).
2a	
	0.31 (3H, d, $J_{HP} = 6.0$ Hz, RuMe), 1.45 (3H, d, $J_{HP} = 8.0$ Hz, PMe), 1.54 (18H, s, C_6Me_6), 7.0–7.6 (15H, m, Ph).
2b	
	0.35 (3H, d, $J_{HP} = 7.1$ Hz, RuMe), 0.99 (3H, $J_{HP} = 8.1$ Hz, PMe), 1.29 (3H, d, $J_{HP} = 8.1$ Hz, PMe), 1.51 (18H, s, C_6Me_6), 7.0–7.6 (10H, m, Ph).
2c	
	0.13 (3H, d, $J_{HP} = 8.1$ Hz, RuMe), 0.84 (9H, d, $J_{HP} = 8.1$ Hz, PMe), 1.65 (18H, s, C_6Me_6), 7.0–7.2 (3H, m, H_m , H_p), 7.3–7.5 (2H, m, H_o).
2d	
	0.25 (3H, d, $J_{HP} = 6.8$ Hz, RuMe), 0.6–1.0 (9H, m, PCH_2Me), 1.2–1.6 (6H, m, PCH_2Me), 1.64 (18H, s, C_6Me_6), 7.0–7.2 (5H, m, Ph).
2e	
	0.40 (3H, d, $J_{HP} = 7.4$ Hz, RuMe), 1.55 (18H, s, C_6Me_6), 2.29 (3H, s, C_6H_4Me), 6.8–7.6 (19H, m, Ph).
m-3a	

Table 1 (continued)

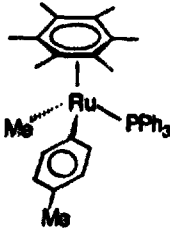
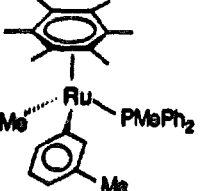
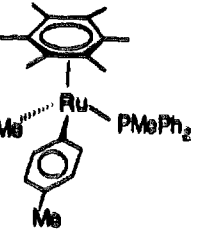
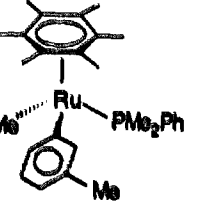
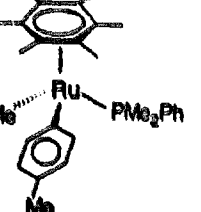
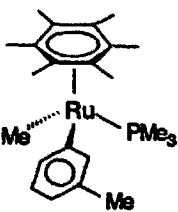
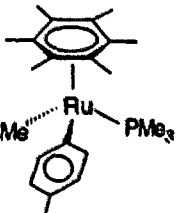
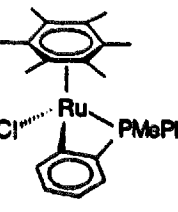
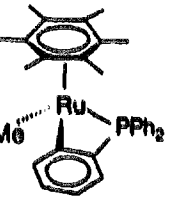
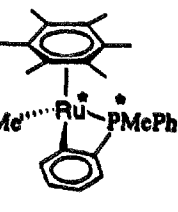
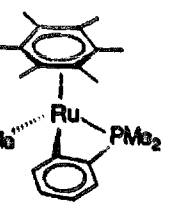
Compound	¹ H NMR
	0.38 (3H, d, $J_{\text{HP}} = 7.4\text{ Hz}$, RuMe), 1.55 (18H, s, C_6Me_6), 2.29 (3H, s, $\text{C}_6\text{H}_4\text{Me}$), 6.8–7.6 (19H, m, Ph).
p-3a	
	0.34 (3H, d, $J_{\text{HP}} = 7.3\text{ Hz}$, RuMe), 1.44 (3H, d, $J_{\text{HP}} = 5.5\text{ Hz}$, PMe), 1.56 (18H, s, C_6Me_6), 2.38 (3H, s, $\text{C}_6\text{H}_4\text{Me}$), 6.9–7.2 (7H, m, Ph), 7.3–7.5 (5H, m, Ph), 7.6–7.7 (2H, m, Ph).
m-3b	
	0.32 (3H, d, $J_{\text{HP}} = 7.3\text{ Hz}$, RuMe), 1.44 (3H, d, $J_{\text{HP}} = 5.5\text{ Hz}$, PMe), 1.56 (18H, s, C_6Me_6), 2.39 (3H, s, $\text{C}_6\text{H}_4\text{Me}$), 6.9–7.2 (7H, m, Ph), 7.3–7.5 (5H, m, Ph), 7.6–7.7 (2H, m, H _a).
p-3b	
	0.36 (3H, d, $J_{\text{HP}} = 7.2\text{ Hz}$, RuMe), 1.02 (3H, d, $J_{\text{HP}} = 8.6\text{ Hz}$, PMe), 1.31 (3H, d, $J_{\text{HP}} = 8.1\text{ Hz}$, PMe), 1.52 (18H, s, C_6Me_6), 2.42 (3H, s, $\text{C}_6\text{H}_4\text{Me}$), 6.9–7.5 (9H, m, Ph).
m-3c	
	0.35 (3H, d, $J_{\text{HP}} = 7.2\text{ Hz}$, RuMe), 1.01 (3H, d, $J_{\text{HP}} = 8.5\text{ Hz}$, PMe), 1.31 (3H, d, $J_{\text{HP}} = 8.1\text{ Hz}$, PMe), 1.52 (18H, s, C_6Me_6), 2.39 (3H, s, $\text{C}_6\text{H}_4\text{Me}$), 6.9–7.5 (9H, m, Ph).
p-3c	

Table 1 (continued)

Compound	¹ H NMR
	0.12 (3H, d, $J_{\text{HP}} = 8.0\text{ Hz}$, RuMe), 0.86 (9H, d, $J_{\text{HP}} = 8.4\text{ Hz}$, PMe), 1.68 (18H, s, C_6Me_6), 2.39 (3H, s, $\text{C}_6\text{H}_4\text{Me}$), 6.9–7.5 (4H, m, Ph).
m-3d	
	0.13 (3H, d, $J_{\text{HP}} = 8.0\text{ Hz}$, RuMe), 0.86 (9H, d, $J_{\text{HP}} = 8.4\text{ Hz}$, PMe), 1.68 (18H, s, C_6Me_6), 2.36 (3H, s, $\text{C}_6\text{H}_4\text{Me}$), 6.9–7.5 (4H, m, Ph).
p-3d	
	A: 1.67 (18H, d, $J_{\text{HP}} = 0.9\text{ Hz}$, C_6Me_6), 1.87 (3H, d, $J_{\text{HP}} = 11.3\text{ Hz}$, PMe), 6.6–7.8 (9H, m, Ph). B: 1.59 (18H, d, $J_{\text{HP}} = 0.6\text{ Hz}$, C_6Me_6), 2.03 (3H, d, $J_{\text{HP}} = 10.1\text{ Hz}$, PMe), 6.6–7.8 (9H, m, Ph).
4a	
	0.19 (3H, d, $J_{\text{HP}} = 7\text{ Hz}$, RuMe), 1.75 (18H, d, $J_{\text{HP}} = 0.7\text{ Hz}$, C_6Me_6), 6.9–7.45 (12H, m, Ph), 7.6–7.85 (2H, m, Ph).
4b	
	A: 0.04 (3H, d, $J_{\text{HP}} = 8.0\text{ Hz}$, RuMe), 1.69 (18H, d, $J_{\text{HP}} = 0.8\text{ Hz}$, C_6Me_6), 6.56–7.80 (9H, m, Ph). B: -0.19 (3H, d, $J_{\text{HP}} = 6.4\text{ Hz}$, RuMe), 1.88 (18H, d, $J_{\text{HP}} = 0.8\text{ Hz}$, C_6Me_6), 6.56–7.80 (9H, m, Ph).
4c	
	0.25 (3H, d, $J_{\text{HP}} = 8\text{ Hz}$, RuMe), 1.08 (3H, d, $J_{\text{HP}} = 9.4\text{ Hz}$, PMe), 1.20 (3H, d, $J_{\text{HP}} = 9.3\text{ Hz}$, PMe), 1.85 (18H, d, $J_{\text{HP}} = 0.7\text{ Hz}$, C_6Me_6), 6.6–7.4 (4H, m, Ph).
4d	

^a If not otherwise specified, spectra were run in C_6D_6 .

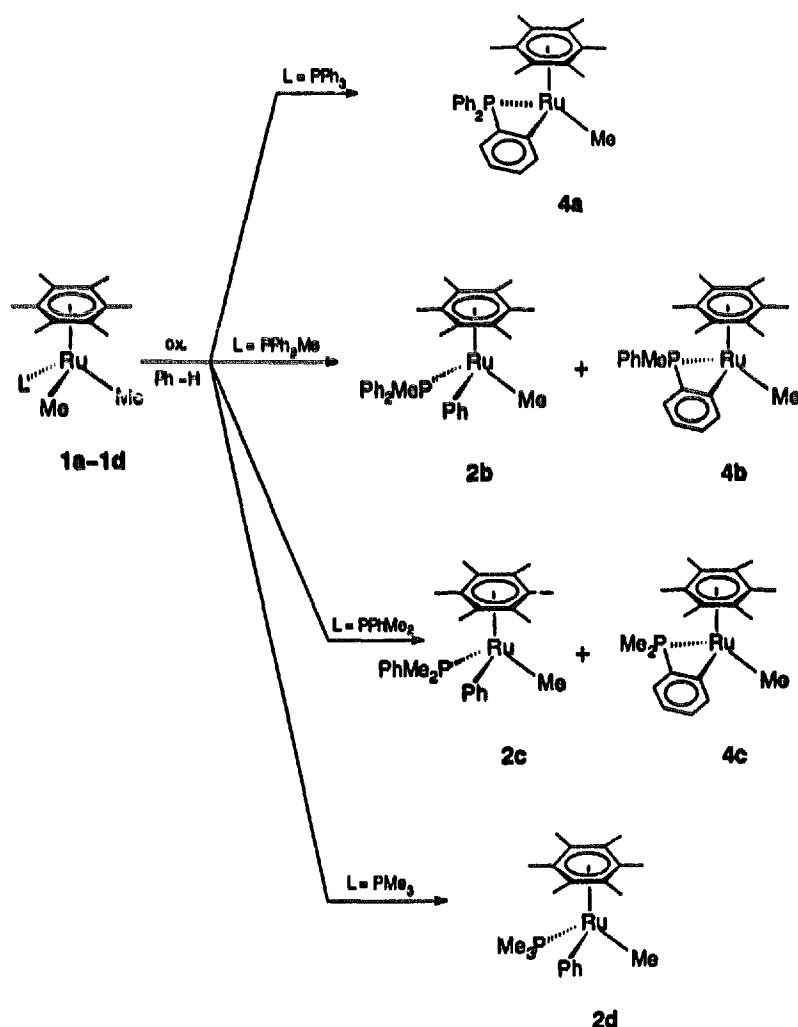
^b In CDCl_3 .

compound, which does not survive the column chromatography on alumina and to which, on the basis of the ^1H NMR resonances at δ 1.61 (18H, s, C_6Me_6) and -0.28 (3H, d, $J_{\text{HP}} = 5.5$ Hz, RuMe), the formula $[\text{Ru}(\text{Me})(\text{X})(\eta^6\text{-C}_6\text{Me}_6)(\text{PPh}_3)]$ can be tentatively assigned, where the identity of X is uncertain. No benzene activation product has been detected, in contrast with the case of the triphenylphosphine-containing iridium system [1–3]. However, **4a** is not stable in the presence of the oxidant, being transformed into $[\text{Ru}(\text{Me})(\text{X})(\eta^6\text{-C}_6\text{Me}_6)(\text{PPh}_3)]$, which is in turn converted by the oxidant into a new compound (δ 1.49) with concurrent formation of methane. The last complex was not isolated, but its ^1H NMR spectrum is apparently consistent with an orthometallated structure.

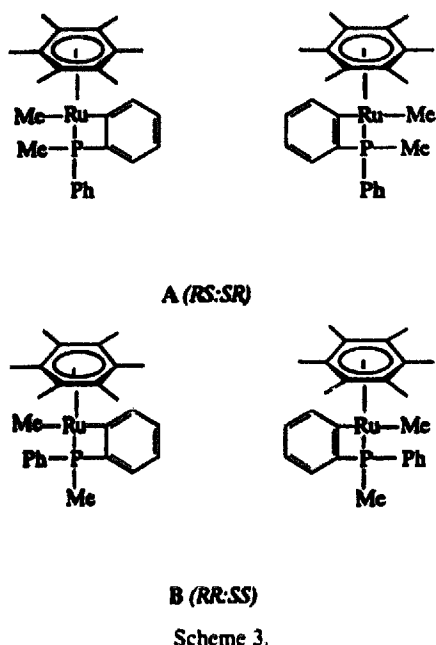
1b and **1c** react in benzene to give mixtures of both intra- and inter-molecular activation products of aromatic C–H bonds, $[\text{Ru}(\text{C}_6\text{H}_4\text{PMePh})(\text{Me})(\eta^6\text{-C}_6\text{Me}_6)]$ (**4b**) (as a 2/1 mixture of two diastereoisomers) and $[\text{Ru}(\text{Me})(\text{Ph})(\eta^6\text{-C}_6\text{Me}_6)(\text{PMePh}_2)]$ (**2b**),

$[\text{Ru}(\text{C}_6\text{H}_4\text{PMe}_2)(\text{Me})(\eta^6\text{-C}_6\text{Me}_6)]$ (**4c**) and $[\text{Ru}(\text{Me})(\text{Ph})(\eta^6\text{-C}_6\text{Me}_6)(\text{PMe}_2\text{Ph})]$ (**2c**) respectively. Attempted chromatographic separation of the diastereomers **4b** was unsuccessful, and the configurations of the major (A) and minor (B) isomers (Scheme 3) were only tentatively attributed on the basis of their ^1H NMR spectra by analogy with the case of $[\text{Ru}(\text{C}_6\text{H}_4\text{PMePh})(\text{CH}_2\text{SiMe}_3)(\eta^6\text{-C}_6\text{Me}_6)]$, whose major isomer was fully characterized as having the (RR:SS) configuration [11]. Finally, **1d** reacts with benzene to give (quantitatively, in 1 h) only $[\text{Ru}(\text{Me})(\text{Ph})(\eta^6\text{-C}_6\text{Me}_6)(\text{PMe}_3)]$ (**2d**), which has been isolated by column chromatography purification followed by crystallization.

These results indicate a strong steric control on the choice between inter- and intra-molecular C–H bond activation: the former prevails as the cone angle of the phosphine decreases, while the latter is favoured when the phosphine is bulky (Table 2), as already observed in the literature [3,12].



Scheme 2.



The above reactions can be described as ETC-catalysed processes of the type already observed for related iridium dimethyl systems [1,2], in which the ferrocenium cation plays the role of a catalytic oxidant: the resulting dimethyl cation activates the C–H bond to give a cationic product which must oxidize the starting complex to close the propagation cycle (see Section 3, Scheme 5).

The data of Table 2 show clearly that the catalysis of the reaction is not very efficient. This cannot be simply due to the insolubility of both the ferrocenium and the intermediate cations (see the analogous reactions of the iridium dimethyl systems [1–3]). Moreover, when the reactions are carried out in arene-CH₂Cl₂ (or in CH₂Cl₂ alone, in those cases where orthometallation of the phosphine may occur), an improvement is observed only for the 1a → 4a reaction, where 73% of 4a is obtained in 1 h. In all the other cases C–H activation was suppressed and only unidentified chlorine-containing products were obtained. We then studied the reaction in neat arenes under heterogeneous conditions.

The yields depend on the amount of [FeCp₂]⁺ (for instance in the case of the 1a → 4a reaction the yield, which after 24 h is 65% by using 30% of catalyst, is reduced to 25% by using 10% of catalyst), but generally speaking the catalytic efficiency is rather low. Very probably, this is due to the relatively low stability of the oxidized complexes, as indicated by the easy release of the hexamethylbenzene ligand, which occurs during the reaction in variable amounts depending on the nature of the phosphine and the experimental conditions (see Table 2). Moreover, when [FeCp₂]PF₆ is added in

amounts larger than stoichiometric, the ¹H NMR signals due to the starting ruthenium complexes gradually disappear and, in solution, only the free hexamethylbenzene remains after 12 h. Another cause of the low efficiency may be due to the formation of side products like the one tentatively identified as [Ru(Me)(X)(η⁶-C₆Me₆)(PPh₃)] in the case of the reaction of 1a.

In the presence of the ferrocenium salt, 1a–1d react also with toluene (Scheme 4): 1a and 1b give only the internal activation products, i.e. the orthometallated complexes 4a and 4b; 1c gives a mixture of the corresponding methyl tolyl and of the orthometallated derivative, and 1d produces only the methyl tolyl complex. As already noted for the thermolysis of 1a–1e in toluene, the ortho positions do not react, and only the meta and para C–H bonds of toluene are activated. Once more, no evidence for benzylic C–H activation has been acquired.

In Table 2 reaction parameters and yields are given.

The fact that from 1b only a 2/1 mixture of diastereisomeric orthometallated complexes has been isolated, without any product of toluene activation, confirms the steric control of the reaction and reflects the growing steric restrictions when toluene is used in place of benzene.

2.4. Electrochemistry of 1a, 1c, 1d, 2b, 2c and coupled EPR measurements

Cyclic voltammetry of complexes 1a, 1c, 1d, 2b, and 2c under inert atmosphere exhibits two sequential anodic processes, of which only the first displays features of chemical reversibility, as illustrated in Fig. 1 for complex 2b.

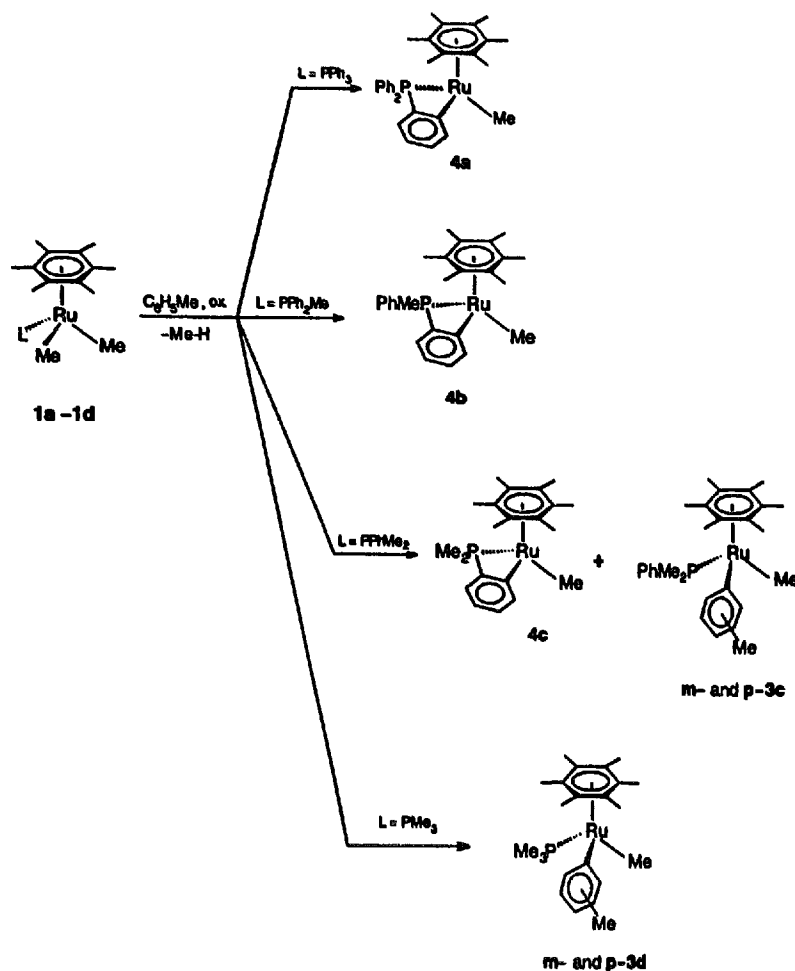
Controlled potential coulometry corresponding to the

Table 2
Experimental data of the oxidatively induced arene activation by [RuMe₂(η⁶-C₆Me₆)(PPh₃)] 1a–1d^a

Complex	Arene	Time (h)	C–H activation products ^b (%)
1a	benzene	24	4a (65)
1b	benzene	24	4b (54), 2b (30)
1c	benzene	24	4c (10), 2c (80)
1d	benzene	15	2d (93)
1a	toluene	3	4a (43)
1b	toluene	24	4b (70)
1c	toluene	3	3c (72), 4c (8)
1d	toluene	18	3d (85)

^a Reactions carried out by using 3 ml of arene, 0.050 g of 1, [FeCp₂]⁺/Ru = 0.3.

^b The difference to 100% includes the decomposition products, as shown by the amounts of free hexamethylbenzene, with the exceptions of the reactions of 1a where two unidentified complexes (ca. 30%) are also present.



Scheme 4.

first anodic step consumes one electron per molecule, and the cyclic voltammogram recorded on the exhaustively oxidized solutions shows a voltammetric profile quite complementary to the original one, but for complexes **1d** and **2c**, the monocations of which undergo slow decomposition reactions. As a typical example, analysis of the cyclic voltammograms of **2b** with scan rates varying from 0.02 to 10.24 V s^{-1} gives evidence for a simple, electrochemically reversible, one-electron transfer ($i_{pc}/i_{pa} = 1$ constantly; $i_{pa} \times v^{-1/2}$ constant; ΔE_p close to 60 mV at low scan rate) [13]. Table 3 compiles the redox potential of the Ru(II)/Ru(III) oxidation of the present complexes, also in comparison with a few related ruthenium derivatives [14,15].

Simple inductive effects of the different substituents account conceivably for the differences in redox potentials.

The formal electrode potential for the neutral/monocation oxidation was not affected by temperature in the range from 258 to 293 K. The fact that the reaction entropy of the Ru(II)/Ru(III) redox couple ΔS_{rc}° is negligible, if any, coupled to the observed electrochemical reversibility, suggests that neither outer-shell nor

inner-shell reorganizations occur as a consequence of the electron removal [16,17].

Owing to the complete irreversibility of the second

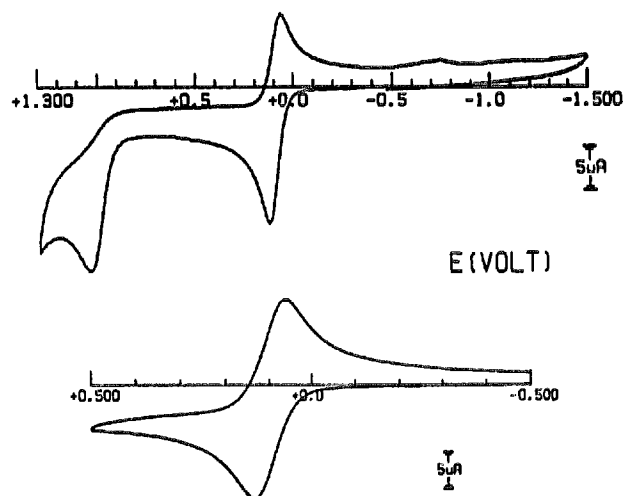


Fig. 1. Cyclic voltammograms recorded at a platinum electrode on a CH_2Cl_2 solution containing **2b** ($1.1 \times 10^{-3} \text{ M}$) and $[NEu_3][ClO_4]$ (0.2 M). Scan rate 0.2 V s^{-1} .

Table 3
Formal electrode potentials for the Ru(II)/Ru(III) couple of some ruthenium complexes

Complex	$E_{(0/+)}^{\circ}$ (V vs. SCE)	ΔE_p^a (mV)	Solvent	Ref.
[RuMe ₂ (η^6 -C ₆ Me ₆ (PPh ₃))] (1a)	0.00	74	CH ₂ Cl ₂	Present work
[RuMe ₂ (η^6 -C ₆ Me ₆ (PMe ₂ Ph))] (1c)	-0.01	72	CH ₂ Cl ₂	Present work
[RuMe ₂ (η^6 -C ₆ Me ₆ (PMe ₃))] (1d)	-0.13	66	CH ₂ Cl ₂	Present work
[Ru(Me)(Ph)(η^6 -C ₆ Me ₆ (PMePh ₂))] (2b)	+0.10	68	CH ₂ Cl ₂	Present work
[Ru(Me)(Ph)(η^6 -C ₆ Me ₆ (PMe ₂ Ph))] (2c)	+0.07	70	CH ₂ Cl ₂	Present work
[RuCp ⁺ (PPh ₃) ₂ (CN)]	+0.57	70	MeCN	[14]
[RuCp ⁺ (PPh ₃)(NO)(CN)] ⁺	-0.30	85	MeCN	[14]
[RuCl ₃ (η^6 -C ₆ Me ₆)]	+0.56 ^b		CH ₂ Cl ₂	[15]

^a Measured at 0.1 V s⁻¹.

^b Followed by fast chemical complications.

anodic step, which could be assigned to the oxidation of the phosphine ligand as well as to the Ru(III)/Ru(IV) step, no further examination of this process was performed.

Fig. 2 shows (a) the first and (b) the second derivatives of the X-band EPR spectra recorded at 100 K on a sample of [2b]⁺ obtained by controlled potential electrolysis at 253 K in dichloromethane solution.

The line-shape analysis shows a broad and unresolved anisotropic spectral pattern, which can be suitably interpreted assuming an $S = 1/2$ spin Hamiltonian in a d^5 low-spin configuration ($\Delta g_{1-h} = g_1 - g_h = 0.204$). The relevant computed anisotropic parameters [18] are collected in Table 4. The $g_1 \neq g_e = 2.0023$



Fig. 2. X-band ESR spectra recorded on a CH₂Cl₂ sample solution of **2b** withdrawn at the first stages of controlled potential electrolysis (0.3 electron/molecule at $E_a = +0.5$ V) performed at 253 K. (a) First derivative spectrum recorded at liquid nitrogen temperature (100 K); (b) second derivative mode.

values test for the metal-in character of the monocation. The absence of hyperfine peaks of the ⁹⁹Ru and ¹⁰¹Ru nuclei ($I = 3/2$ and $5/2$ respectively) and of the ³¹P nucleus likely arises from the actual glassy state line-width, and from the expected geometrical distortions experienced by the tetrahedral coordinating polyhedron. Then, the following upper limit for the direct magnetic interaction of the unpaired electron with the phosphorus nucleus of the phosphine can be proposed:

$$a_{i(^{31}\text{P})} \leq \Delta H_i = 45 \pm 3 \text{ G}; a_{m(^{31}\text{P})} \leq \Delta H_m = 35 \pm 3 \text{ G};$$

$$a_h(^{31}\text{P}) \leq \Delta H_h = 30 \pm 3 \text{ G}$$

The anisotropic spectrum drops out at the glassy-fluid transition phase, and the paramagnetic [2b]⁺ species becomes EPR silent in the overall fluid solution temperature range, likely as a consequence of the dynamically fastened paramagnetic relaxation mechanisms. Upon refreezing, the rhombic signal appears again.

[2c]⁺ exhibits quite similar EPR paramagnetic features with a more marked separation, $\Delta g_{1-h} = 0.221$, which could be assigned to an increased distortion of the tetrahedral geometry. Its fluid solution ($T = 215$ K) displays a broad and unresolved isotropic signal with $g_{av(215\text{ K})} = 2.130 \pm 0.008$ and $\Delta H_{av(215\text{ K})} = 240 \pm 10$ G, well fitting the glassy g_1 values. The broad signal disappears at higher temperatures, due to the increasing spectral width, and it restores upon refreezing.

[1a]⁺ and [1d]⁺ display X-band paramagnetic features very similar to those previously discussed for [2b]⁺ and [2c]⁺, even if in the presence of less pronounced rhombic features, likely correlated to the higher symmetry of complexes [1a]⁺ and [1d]⁺ (C_s symmetry). Accordingly, the fluid solution ($T = 215$ K) of [1d]⁺ exhibits an unresolved absorption ($\Delta H_{av(215\text{ K})} = 150 \pm 10$ G, $g_{av} = 2.133 \pm 0.008$) less broad than that of [2c]⁺.

Finally, we would like to underline that we have been unable to induce electrochemically the chemically induced catalytic conversion of **1a** and **1b** to the or-

Table 4
X-band EPR parameters for the Ru(III) complexes

Complex	g_1^a	g_m^a	g_h^a	$\langle g \rangle^b$	$g_{av}^{c,d}$	Δg_{1-h}^c
1a	2.205	2.180	2.021	2.135	—	0.184
1d	2.199	2.177	2.005	2.127	2.133	0.194
2b	2.215	2.185	2.010	2.136	— ^c	0.205
2c	2.222	2.186	2.001	2.136	2.130	0.221

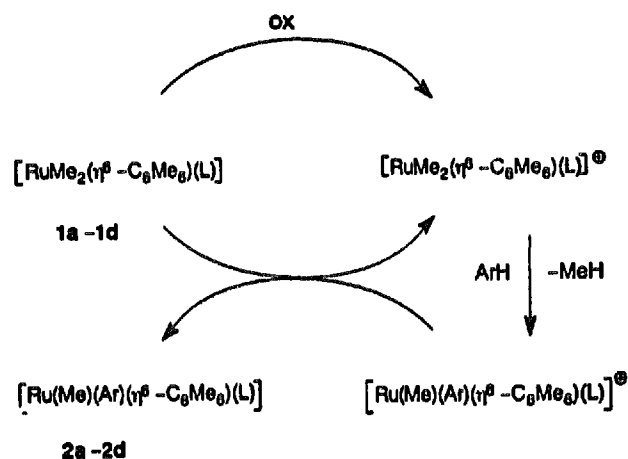
^a ± 0.003 . ^b $\langle g \rangle = (g_1 + g_m + g_h)/3$. ^c ± 0.008 . ^d $T = 215$ K. ^e Silent.

thometallated derivatives (**4a** and **4b** respectively) via loss of methane.

3. Conclusions

The dimethyl complexes $[\text{Ru}(\text{Me})_2(\eta^6\text{-C}_6\text{Me}_6)(\text{PR}_3)]$ **1a–1d** have been found to react with benzene and toluene C–H bonds only under rather severe conditions, but, in the presence of ferrocenium, their reactivity increases greatly. This behaviour is analogous to that observed for the isoelectronic iridium systems $[\text{IrMe}_2\text{Cp}^*(\text{PR}_3)]$ [1–3], which have been found to react according to an electron transfer catalysis, and suggests the generality of such an approach to the ‘ σ -bond metathesis’ reaction of M–C and arene C–H bonds. Following the electron transfer chain mechanistic scheme [19], the ruthenium species $[\text{Ru}(\text{Me})_2(\eta^6\text{-C}_6\text{Me}_6)(\text{PR}_3)]^+$, deriving from the one-electron oxidation of **1a–1d**, reacts with arenes to yield a cationic ruthenium(III) derivative; this in turn oxidizes **1a–1d** giving rise to the final methyl aryl products **2a–2d** (Scheme 5).

Most of the examples reported in the literature [19] have quite exergonic cross-propagation steps, and are fast and complete. In our case the potentials for the $1/1^+$ and $2/2^+$ couples are probably not that different (as judged from the 80 mV difference in the case of **1c** and **2c**, Table 3); therefore, most of the driving force of the reaction is likely to arise from the formation of methane.



Scheme 5.

The increased reactivity of the ruthenium systems under electron transfer conditions could most probably be related to the formation of the ‘open sphere’ 17-electron ruthenium systems $[\mathbf{1a}]^+–[\mathbf{1d}]^+$ [20], which are more prone towards arene coordination than the saturated **1a–1d**. Accordingly, as already reported for the iridium systems [1–3], activation of aromatic phosphines to the orthometallated derivatives has not been observed under thermal conditions which require the loss of a ligand (most probably the phosphine).

Electrochemical investigation does confirm the easy oxidation of the dimethyl ruthenium complexes, but, as in the iridium case, different results are obtained by electrochemical or chemical oxidation: for instance, voltammetric techniques in CH_2Cl_2 show that the electrochemically generated $[\mathbf{1a}]^+$ does not produce the orthometallated complex **4a**; this is in contrast with the results of the reaction of **1a** in the same solvent in the presence of $[\text{FeCp}_2]\text{PF}_6$.

This is surprising, but is quite analogous to what has been observed for the reactions of the related iridium systems [2]. In those cases, ESR spectroscopy has shown that the oxidation of the dimethyl systems under electrochemical and chemical oxidation produces two different types of cation, which have different fates. This behaviour was interpreted as due to two different oxidation mechanisms: an inner-sphere mechanism for the chemical oxidation, and an outer-sphere for the electrochemical oxidation; this is what we suggest for the ruthenium complexes too.

As for the intimate mechanism of these C–H activation reactions, some evidence seems to indicate a similarity between the iridium, ruthenium and early transition metal systems. Therefore, in the absence of detailed mechanistic studies, we are inclined to embrace the hypothesis of a four-centre transition state as proposed for the ‘ σ -bond metathesis’ of C–H and M–C bonds by scandocene systems [4].

4. Experimental section

The reactions and manipulation of organometallics were carried out under dinitrogen or argon, using standard techniques. The solvents were dried and distilled

prior to use. The compounds $[\text{Ru}(\text{Cl})_2(\eta^6\text{-C}_6\text{Me}_6)(\text{PPh}_3)]$, $[\text{Ru}(\text{Cl})_2(\eta^6\text{-C}_6\text{Me}_6)(\text{PMePh}_2)]$, $[\text{Ru}(\text{Cl})_2(\eta^6\text{-C}_6\text{Me}_6)(\text{PMe}_3)]$ were prepared according to literature procedures [7]. $[\text{FeCp}_2]\text{PF}_6$ and AgBF_4 were Aldrich products. The ^1H NMR spectra were recorded using Varian Gemini 200 or VXR 300 spectrometers, operating respectively at 200 MHz and 300 MHz. The ^1H NMR chemical shifts were referenced to residual protiated solvent as follows: benzene- d_6 $\delta = 7.15$, dichloromethane- d_2 $\delta = 5.32$. The ^{31}P spectra were recorded on the VXR-300 instrument at 121 MHz and the chemical shifts were referred to H_3PO_4 (external standard). Materials and methods for electrochemistry and EPR spectroscopy of the electrogenerated species have been described elsewhere [21]. All potential values are referred to the saturated calomel electrode (SCE). Under the present experimental conditions, the one-electron oxidation of ferrocene occurs at $E^\circ = +0.44\text{ V}$ in CH_2Cl_2 and at $E^\circ = +0.54\text{ V}$ in THF solutions. A non-isothermal cell assembly was used for cyclic voltammetry at variable temperature [22]. X-band EPR spectra were computed by the SIM14a computer simulation program [18]. Elemental analyses were performed by the Laboratorio di Microanalisi of the Istituto di Chimica Organica, Facoltà di Farmacia, University of Pisa.

4.1. Preparation of $[\text{Ru}(\text{Cl})_2(\eta^6\text{-C}_6\text{Me}_6)(\text{PMe}_2\text{Ph})]$

A solution of $[\text{Ru}(\text{Cl})_2(\eta^6\text{-C}_6\text{Me}_6)]_2$ (0.948 g, 1.42 mmol) and dimethylphenylphosphine (0.8 ml, 5.68 mmol) in 35 ml of chloroform was refluxed for 6 h. After concentration to half volume, addition of hexane (60 ml) caused the precipitation of red-brown crystals. The solid was washed with hexane and dried in vacuo. Yield: 1.206 g (90%). Anal. Found: C, 50.2; H, 5.9. $\text{C}_{20}\text{H}_{20}\text{Cl}_2\text{PRu}$. Calc.: C, 50.8; H, 6.2%.

4.2. Preparation of $[\text{Ru}(\text{Cl})_2(\eta^6\text{-C}_6\text{Me}_6)(\text{PEt}_3)]$

Following the same procedure $[\text{Ru}(\text{Cl})_2(\eta^6\text{-C}_6\text{Me}_6)]_2$ (1.6 g, 2.39 mmol) and triethylphosphine (1.38 ml, 9.324 mmol) were reacted in chloroform (70 ml) to give 2.133 g of a red-brown product (98%). Anal. Found: C, 47.0; H, 7.8. $\text{C}_{18}\text{H}_{16}\text{Cl}_2\text{PRu}$. Calc.: C, 47.5; H, 8.0%.

4.3. Preparation of $[\text{Ru}(\text{Me})_2(\eta^6\text{-C}_6\text{Me}_6)(\text{PPh}_3)]$ (**1a**)

$[\text{Ru}(\text{Cl})_2(\eta^6\text{-C}_6\text{Me}_6)(\text{PPh}_3)]$ (0.367 g, 0.62 mmol) in benzene (20 ml) was reacted with LiMe (3.85 ml of a 1.6 M solution in diethyl ether, 6.16 mmol) for 14 h at room temperature. The mixture was hydrolysed at 0°C with water, the organic phase was separated and dried under vacuum. The solid residue was dissolved in benzene (5 ml), and chromatographed on alumina column ($h = 7\text{ cm}$) using benzene as the eluant. The yellow

band was dried under vacuum to give 0.173 g (51%) of an orange-yellow solid, having the same ^1H NMR spectrum reported in the literature for an authentic sample [7].

4.4. Preparation of $[\text{Ru}(\text{Me})_2(\eta^6\text{-C}_6\text{Me}_6)(\text{PMePh}_2)]$ (**1b**)

Following the same procedure as above, $[\text{Ru}(\text{Cl})_2(\eta^6\text{-C}_6\text{Me}_6)(\text{PMePh}_2)]$ (0.36 g, 0.67 mmol) in benzene (20 ml) was treated with LiMe (4.2 ml of a 1.6 M solution in diethyl ether, 6.72 mmol). After 14 h the mixture was hydrolysed at 0°C with water, and the organic phase dried under vacuum. By column chromatography on alumina of the orange-yellow residue with benzene, and evaporation of the solvent, an orange-yellow solid was obtained (0.115 g, 35%), which was identified as **1b** by comparison with the spectra reported in the literature [7]. ^1H NMR (benzene- d_6): δ 0.06 (6H, dd, $J_{\text{HP}} = 6.1\text{ Hz}$, RuMe), 1.56 (18H, s, C_6Me_6), 1.65 (3H, d, $J_{\text{HP}} = 3.9\text{ Hz}$, PMe), 7–7.15 (6H, m, $\text{H}_m + \text{H}_p$), 7.3–7.45 (4 H, m, H_o).

4.5. Preparation of $[\text{Ru}(\text{Me})_2(\eta^6\text{-C}_6\text{Me}_6)(\text{PMe}_2\text{Ph})]$ (**1c**)

$[\text{Ru}(\text{Cl})_2(\eta^6\text{-C}_6\text{Me}_6)(\text{PMe}_2\text{Ph})]$ (0.435 g, 0.92 mmol) in diethyl ether (20 ml) was reacted with LiMe (5.7 ml of a 1.6 M solution in diethyl ether, 9.12 mmol). After 14 h the suspension was hydrolysed and the organic layer was dried over sodium sulphate. The crude product was transferred to the top of an alumina chromatography column ($h = 4\text{ cm}$). Benzene eluted a band from which the pure dimethyl derivative as orange-yellow microcrystals was recovered (0.183 g, 46%). Anal. Found: C, 60.9; H, 8.3; P, 7.0. $\text{C}_{22}\text{H}_{15}\text{PRu}$. Calc.: C, 61.2; H, 8.1; P, 7.2%.

4.6. Preparation of $[\text{Ru}(\text{Me})_2(\eta^6\text{-C}_6\text{Me}_6)(\text{PMe}_3)]$ (**1d**)

Following the above procedure $[\text{Ru}(\text{Cl})_2(\eta^6\text{-C}_6\text{Me}_6)(\text{PMe}_3)]$ (0.269 g, 0.66 mmol) in diethyl ether (20 ml) was reacted with LiMe (4.1 ml of a 1.6 M diethyl ether solution, 6.56 mmol) for 14 h. The usual work-up and column chromatography ($h = 2\text{ cm}$) purification gave 0.142 g of **1d** as a yellow solid (59%), characterized by comparison with the literature data [7]. ^1H NMR (benzene- d_6): δ -0.13 (6H, d, $J_{\text{HP}} = 7\text{ Hz}$, RuMe), 0.96 (9H, d, $J_{\text{HP}} = 8.2$, PMe), 1.73 (18H, s, C_6Me_6).

4.7. Preparation of $[\text{Ru}(\text{Me})_2(\eta^6\text{-C}_6\text{Me}_6)(\text{PEt}_3)]$ (**1e**)

Reaction of $[\text{Ru}(\text{Cl})_2(\eta^6\text{-C}_6\text{Me}_6)(\text{PEt}_3)]$ (0.365 g, 0.87 mmol) in diethyl ether (20 ml) with PhMgBr (5.4 ml of a 1.6 M solution in diethyl ether, 8.64 mmol) gave

yellow-green microcrystals of **1e** (0.189 g, 53% yield). Anal. Found: C, 58.0; H, 9.6; P, 7.1. $C_{20}H_{39}PRu$. Calc.: C, 58.4; H, 9.5; P, 7.5%.

4.8. Preparation of $[Ru(Cl)(Ph)(\eta^6-C_6Me_6)(PMePh_2)]$

A suspension of $[Ru(Cl)_2(\eta^6-C_6Me_6)(PMePh_2)]$ (0.350 g, 0.65 mmol) in diethyl ether (10 ml) was reacted overnight with $PhMgBr$ (2 ml of a 1.6 M solution in diethyl ether, 3.2 mmol). Hydrolysis gave an ethereal solution which was pumped to dryness to give a residue which was chromatographed on an alumina column (benzene as eluant) to give orange microcrystals (0.056 g, 15% yield). Anal. Found: C, 64.2; H, 6.1. $C_{31}H_{36}ClPRu$. Calc.: C, 64.6; H, 6.3%.

4.9. Preparation of $[Ru(Cl)(Ph)(\eta^6-C_6Me_6)(PEt_3)]$

By the same procedure as above $[RuCl_2(\eta^6-C_6Me_6)(PEt_3)]$ (0.250 g, 0.55 mmol) was reacted with $PhMgBr$ (1.8 ml of a 1.6 M diethyl ether solution, 2.8 mmol) to give orange crystals (0.033 g, 12%). Anal. Found: C, 57.9; H, 7.7. $C_{24}H_{38}ClPRu$. Calc.: C, 58.3; H, 7.8%.

4.10. Preparation of $[Ru(Me)(Ph)(\eta^6-C_6Me_6)(PPh_3)]$ (**2a**)

A suspension of $[Ru(Cl)_2(\eta^6-C_6Me_6)(PPh_3)]$ (0.318 g, 0.53 mmol) in diethyl ether (20 ml) was added with $PhMgBr$ (0.89 ml of a 3 M solution in diethyl ether, 2.67 mmol), and stirred at room temperature for 20 h. After hydrolysis at 0°C with water, the organic phase was dried and evaporated to give 0.112 g of an orange-red solid, which was dissolved in diethyl ether (20 ml) and reacted with $LiMe$ (1.2 ml of a 1.6 M diethyl ether solution, 1.92 mmol). The mixture was stirred at room temperature for 20 h and then hydrolysed at 0°C with water. The organic phase was evaporated to dryness, and the residue was chromatographed on a column of alumina. Pentane–benzene 1:1 eluted a yellow band which gave orange-yellow crystals of $[RuMe(Ph)(\eta^6-C_6Me_6)(PPh_3)]$ (0.039 g, 12% yield). Anal. Found: C, 72.3; H 6.4. $C_{37}H_{41}PRu$. Calc.: C, 72.0; H, 6.6%. ^{31}P NMR (benzene- d_6): δ 54.78.

4.11. Preparation of $[Ru(Me)(Ph)(\eta^6-C_6Me_6)(PMePh_2)]$ (**2b**)

By the same procedure as above, $[Ru(Cl)_2(\eta^6-C_6Me_6)(PMePh_2)]$ (0.303 g, 0.57 mmol) in diethyl ether (20 ml) was reacted with $PhMgBr$ (0.95 ml of a 3 M solution in diethyl ether, 2.85 mmol) and then with $LiMe$ (3.5 ml of a 1.6 M diethyl ether solution, 5.7 mmol) to give 0.025 g of the orange-yellow compound **2b** (8%). Anal. Found: C, 69.5; H, 7.1. $C_{32}H_{39}PRu$. Calc.: C, 69.2; H, 7.0%. ^{31}P NMR (benzene- d_6): δ 35.78.

4.12. Preparation of $[Ru(Me)(Ph)(\eta^6-C_6Me_6)(PMe_2Ph)]$ (**2c**)

By the same procedure as above, $[Ru(Cl)_2(\eta^6-C_6Me_6)(PMe_2Ph)]$ (0.271 g, 0.58 mmol) in diethyl ether (20 ml) was reacted with $PhMgBr$ (0.96 ml of a 3 M solution in diethyl ether, 2.9 mmol) and then with $LiMe$ (3.6 ml of a 1.6 M diethyl ether solution, 5.7 mmol) to give 0.017 g of orange-yellow product (6%). Anal. Found: C, 65.1; H, 7.3. $C_{27}H_{37}PRu$. Calc.: C, 65.7; H, 7.5%.

4.13. Preparation of $[Ru(Me)(Ph)(\eta^6-C_6Me_6)(PEt_3)]$ (**2e**)

By the same procedure as above, $[Ru(Cl)_2(\eta^6-C_6Me_6)(PEt_3)]$ (0.330 g, 0.73 mmol) was reacted with $PhMgBr$ (1.22 ml of a 3 M solution in diethyl ether, 3.65 mmol) and then with $LiMe$ (4.5 ml of a 1.6 M diethyl ether solution, 7.2 mmol) to give 0.023 g of orange-yellow product (7.2%). Anal. Found: C, 62.9; H, 8.8. $C_{25}H_{41}PRu$. Calc.: C, 63.4; H, 8.7%.

4.14. Thermolysis of **1a–1e** in benzene

1a (0.02 g) and benzene (1 ml), or benzene- d_6 when monitoring the reaction by 1H NMR spectroscopy, were loaded into an NMR tube and the tube was sealed off under argon. The tube was immersed in a thermostatted oil bath. The progress of the reaction was evaluated by monitoring the signal of CH_3D (δ 0.13 (t, $J_{HD} = 2$ Hz)), and the integrated intensities of the C_6Me_6 resonances for **2a**. After heating **1a** in benzene for 75 h at 85°C, the tube was cracked open, the solvent was removed, and benzene- d_6 was added and the resulting products examined by 1H NMR analysis. The following yields have been obtained: **2a-d₅** (60%, 50 h, 85°C), **2b-d₅** (37%, 250 h, 85°C), **2c-d₅** (37%, 250 h, 100°C), **2d-d₅** (20%, 220 h, 110°C), **2e-d₅** (53%, 300 h, 85°C).

4.15. General procedure for the reaction of **1a–1d** with $[FeCp_2]PF_6$ in benzene

The same procedure was used for the reactions of **1a–1d**. The reaction of **1a** is described as an example.

1a (0.054 g, 0.098 mmol) and $[FeCp_2]PF_6$ (1.1 mg, 0.0032 mmol) were reacted in benzene (3 ml) or, when monitoring the reaction by 1H NMR spectroscopy, in benzene- d_6 using hexamethylbenzene as internal standard. CH_4 (δ 0.14) was evolved and **1a** was quantitatively converted after 24 h to a mixture of the orthometallated compound **4a** (65% yield) and of an unidentified compound (18%). **4a** was purified by column chromatography on alumina: elution with pentane–benzene (1:1) gave a yellow solid. Anal. Found: C, 68.8; H, 6.6.

$C_{31}H_{35}PRu$. Calc.: C, 69.0; H, 6.5%. ^{31}P NMR (benzene- d_6): δ –10.8.

4.16. Reaction of (1a)–(1d) with $[FeCp_2]PF_6$ in toluene: general procedure

The reactions were carried out following the same procedure described for the analogous reactions in benzene.

Acknowledgements

We thank CNR (Rome) and MURST (Rome) for financial support.

References

- [1] P. Diversi, S. Iacononi, G. Ingrosso, F. Laschi, A. Lucherini and P. Zanello, *J. Chem. Soc. Dalton Commun.*, (1993) 351.
- [2] P. Diversi, S. Iacononi, G. Ingrosso, F. Laschi, A. Lucherini, C. Pinzino, G. Uccello-Barretta and P. Zanello, *Organometallics*, **14** (1995) 3275.
- [3] F. de Biani Fabrizi, P. Diversi, G. Ingrosso, F. Laschi, A. Lucherini, C. Pinzino, G. Uccello-Barretta and P. Zanello, *Gazz. Chim. Ital.*, **126** (1996) 391.
- [4] (a) P.L. Watson and G.W. Parshall, *Acc. Chem. Res.*, **18** (1985) 51. (b) C.M. Fendrick and T.J. Marks, *J. Am. Chem. Soc.*, **108** (1986) 425. (c) M.E. Thompson, S.E. Baxter, A. Ray Bulls, B.J. Burger, M.C. Nolan, B.D. Santarsiero, W.P. Schaefer and J.E. Bercaw, *J. Am. Chem. Soc.*, **109** (1987) 203. (d) I.P. Rothwell, in C.L. Hill (ed.), *Activation and Functionalization of Alkanes*, Wiley, New York, 1989, p. 151.
- [5] M. Gomez, P.I. Yarrow, D.J. Robinson and P.M. Maitlis, *J. Organomet. Chem.*, **279** (1985) 115.
- [6] (a) H. Lehmkuhl, M. Bellenbaum and J. Grundke, *J. Organomet. Chem.*, **330** (1987) C23. (b) H. Lehmkuhl, M. Bellenbaum, J. Grundke, H. Mauermann and C. Krüger, *Chem. Ber.*, **121** (1988) 1719. (c) H. Lehmkuhl, R. Schwickardi, G. Mehler, C. Krüger and R. Goddard, *Z. Anorg. Allg. Chem.*, **606** (1991) 141.
- [7] H. Werner and H. Kletzin, *J. Organomet. Chem.*, **228** (1982) 289.
- [8] V. Adovasio, P. Diversi, G. Ingrosso, A. Lucherini, F. Marchetti and M. Nardelli, *J. Chem. Soc. Dalton Trans.*, (1992) 3385.
- [9] C.A. Tolman, *Chem. Rev.*, **77** (1977) 313. Md.M. Rahman, H.-Y. Liu, K. Eriks, A. Prock and W.P. Giering, *Organometallics*, **8** (1989) 1.
- [10] P.E. Garrou, *Chem. Rev.*, **81** (1981) 229.
- [11] P. Diversi, G. Ingrosso, A. Lucherini, F. Marchetti, V. Adovasio and M. Nardelli, *J. Chem. Soc. Dalton Trans.*, (1990) 1779. P. Diversi, G. Ingrosso, A. Lucherini, F. Marchetti, V. Adovasio and M. Nardelli, *J. Chem. Soc. Dalton Trans.*, (1991) 203.
- [12] (a) W.D. Jones and F.J. Feher, *J. Am. Chem. Soc.*, **106** (1984) 650. (b) W.D. Jones and F.J. Feher, *J. Am. Chem. Soc.*, **107** (1985) 620. (c) T.T. Wenzel and R.G. Bergman, *J. Am. Chem. Soc.*, **108** (1986) 4856. (d) W.D. Jones, in C.L. Hill (ed.), *Activation and Functionalization of Alkanes*, Wiley, New York, 1989, p. 111.
- [13] E.R. Brown and J. Sandifer, in B.W. Rossiter and J.F. Hamilton (eds.), *Physical Methods of Chemistry. Electrochemical Methods*, Vol. 2, Wiley, New York, 1986, Chapter 4.
- [14] W.M. Laidlaw and R.G. Denning, *J. Organomet. Chem.*, **463** (1993) 199.
- [15] U. Kölle, R. Görissen and A. Hörmig, *Inorg. Chim. Acta*, **218** (1994) 33.
- [16] D.E. Richardson and P. Sharpe, *Inorg. Chem.*, **32** (1993) 1809. P.W. Crawford and F.A. Schultz, *Inorg. Chem.*, **33** (1994) 4344.
- [17] P. Zanello, in P. Zanello (ed.), *Stereochemistry of Organometallic and Inorganic Compounds*, Vol. 5, Elsevier, Amsterdam, 1994, p. 163.
- [18] J.P. Lozos, B.M. Hoffmann and C.G. Franz, *QCPE*, **11** (1973) 243.
- [19] M. Chanon and M.L. Tobe, *Angew. Chem. Int. Ed. Engl.*, **21** (1982) 1. D. Astruc, *Angew. Chem. Int. Ed. Engl.*, **27** (1988) 643.
- [20] D.R. Tyler, *Prog. Inorg. Chem.*, **36** (1988) 125. D.R. Tyler, *Acc. Chem. Res.*, **24** (1991) 325.
- [21] D. Osella, M. Ravera, C. Nervi, C.E. Housecroft, P.R. Raithby, P. Zanello and F. Laschi, *Organometallics*, **10** (1991) 3253.
- [22] E.L. Yee, R.J. Cuve, K.L. Guyer, P.D. Tyma and M.J. Weaver, *J. Am. Chem. Soc.*, **101** (1979) 1131.